Epilepsy Research (2014) **108**, 1511—1518

journal homepage: www.elsevier.com/locate/epilepsyres

Characterization of a *de novo SCN8A* mutation in a patient with epileptic encephalopathy

Carolien G.F. de Kovel[a,*], Miriam H. Meisler[c,d], Eva H. Brilstra[a], Frederique M.C. van Berkestijn[b], Ruben van 't Slot[a], Stef van Lieshout[a], Isaac J. Nijman[a], Janelle E. O'Brien[c], Michael F. Hammer[g], Mark Estacion[e,f], Stephen G. Waxman[e,f], Sulayman D. Dib-Hajj[e,f], Bobby P.C. Koeleman[a]

[a] *Department of Medical Genetics, University Medical Center Utrecht, Utrecht, The Netherlands*
[b] *Department of Pediatrics, University Medical Center Utrecht, Utrecht, The Netherlands*
[c] *Department of Human Genetics, University of Michigan, Ann Arbor, MI 48109-5618, USA*
[d] *Department of Neurology, University of Michigan, Ann Arbor, MI 48109-5618, USA*
[e] *Department of Neurology, Center for Neuroscience and Regeneration Research, Yale University School of Medicine, New Haven, CT 06510, USA*
[f] *Rehabilitation Research Center, Veterans Affairs Connecticut Healthcare System, West Haven, CT 06516, USA*
[g] *Arizona Research Laboratories, Division of Biotechnology, University of Arizona, Tucson, AZ 85721, USA*

Received 28 January 2014; received in revised form 19 May 2014; accepted 26 August 2014
Available online 4 September 2014

KEYWORDS
SCN8A;
Nav1.6;
Epileptic encephalopathy;
Exome sequencing;
Patch-clamp

Summary
Objective: Recently, *de novo SCN8A* missense mutations have been identified as a rare dominant cause of epileptic encephalopathies (EIEE13). Functional studies on the first described case demonstrated gain-of-function effects of the mutation. We describe a novel *de novo* mutation of *SCN8A* in a patient with epileptic encephalopathy, and functional characterization of the mutant protein.
Design: Whole exome sequencing was used to discover the variant. We generated a mutant cDNA, transfected HEK293 cells, and performed Western blotting to assess protein stability. To study channel functional properties, patch-clamp experiments were carried out in transfected neuronal ND7/23 cells.
Results: The proband exhibited seizure onset at 6 months of age, diffuse brain atrophy, and more profound developmental impairment than the original case. The mutation p.Arg233Gly

* Corresponding author. Tel.: +31 88 7568297; fax: +31 88 7568479.
E-mail address: c.dekovel@umcutrecht.nl (C.G.F. de Kovel).

http://dx.doi.org/10.1016/j.eplepsyres.2014.08.020

in the voltage sensing transmembrane segment D1S4 was present in the proband and absent in both parents. This mutation results in a temperature-sensitive reduction in protein expression as well as reduced sodium current amplitude and density and a relative increased response to a slow ramp stimulus, though this did not result in an absolute increased current at physiological temperatures.

Conclusion: The new *de novo SCN8A* mutation is clearly deleterious, resulting in an unstable protein with reduced channel activity. This differs from the gain-of-function attributes of the first *SCN8A* mutation in epileptic encephalopathy, pointing to heterogeneity of mechanisms. Since Nav1.6 is expressed in both excitatory and inhibitory neurons, a differential effect of a loss-of-function of Nav1.6 Arg223Gly on inhibitory interneurons may underlie the epilepsy phenotype in this patient.

Introduction

Among the known epilepsy genes, brain-expressed voltage-gated sodium channels are currently the most clinically relevant, with a large number of mutations detected in patients suffering from various epileptic disorders, the majority in *SCN1A* (Mulley et al., 2005), smaller numbers in *SCN2A* (Shi et al., 2012), and a few in other channels (Meisler et al., 2010). The association of voltage-gated sodium channels with epilepsy displays both clinical and genetic heterogeneity. Dominant mutations in both *SCN1A* and *SCN2A* have been found in severe as well as milder epileptic disorders: MIM607208 and MIM604403, and MIM613721 and MIM607745 respectively. A strong, yet incomplete, correlation exists between mutation type (*i.e.* missense or nonsense) and the corresponding epilepsy phenotype (Scheffer et al., 2009). For example, nonsense mutations in *SCN1A* are predominantly found in Dravet syndrome patients, which predict a loss of function of one allele and haploinsufficiency as the main disease mechanism. On the other hand, missense mutations are predominantly found in GEFS+ patients, suggesting a gain of function effect underlying this milder form of epilepsy. The variety in effects of mutations in these sodium channel genes underscores the importance of careful phenotype *versus* genotype and molecular phenotype comparisons to elucidate the clinical relevance of sodium channel mutations (Meisler and Kearney, 2005).

In 2012, the *de novo* mutation p.Asn1768Asp in *SCN8A* (encoding Nav1.6) was reported in a child with infantile epileptic encephalopathy (EE) and SUDEP (Veeramah et al., 2012). The authors showed that the functional effect of the mutation, an increase in persistent current, was consistent with a dominant, gain-of-function phenotype (Veeramah et al., 2012), suggesting that gain-of-function mutations of *SCN8A* can underlie EE. Earlier, an inherited loss of function mutation caused by a 2 bp deletion (Pro1719ArgfsX6) (Supp. Fig. A1) had been reported as a possible cause for cerebellar ataxia and cognitive problems (Meisler and Kearney, 2005; Trudeau et al., 2006). Recently, seven additional potentially pathogenic mutations in *SCN8A* were reported in patients with intellectual disability and seizures (Carvill et al., 2013; Epi4K-Consortium, 2013; Rauch et al., 2012; Vaher et al., 2013) (Supp. Fig. A1). Four were demonstrated to be *de novo*, one was inherited from an asymptomatic mosaic father, and for two the inheritance was not known. All reported *de novo* mutations in patients with epileptic encephalopathy so far are missense mutations changing a conserved amino acid, but no further electrophysiological analyses have been published (O'Brien and Meisler, 2013). These observations establish dominant missense mutations in *SCN8A* as a cause of EE (EIEE13), but functional characterization of additional mutations is required to determine the general disease mechanism.

We detected a *de novo* mutation in *SCN8A* (c.667A > G) in a girl with epileptic encephalopathy and secondary microcephaly. In this paper, we report a clinical description of our new case and functional properties of the new mutation (Nav1.6-p.Arg223Gly) and compared them to the previously characterized *de novo* mutation (Veeramah et al., 2012).

Methods

Mutation detection

Whole exome sequencing was performed on genomic DNA from both the parents and the affected child from six trios. Laboratory and bioinformatics procedures were carried out as previously described (Nijman et al., 2010). Candidate *de novo* variants that were predicted to alter protein function were sequenced in fresh DNA aliquots with Sanger sequencing. We also looked for homozygous or compound heterozygous mutations that could be a plausible cause of the disorder.

Generation and expression of the mutant cDNA

The c.667A > G nucleotide mutation was introduced into the tetrodotoxin (TTX)-resistant derivative of the murine Nav1.6 cDNA clone Nav1.6$_R$ as previously described (Sharkey et al., 2009). Mouse *Scn8a* is an appropriate model for human *SCN8A*, since the human and mouse proteins are 99% identical in amino acid sequence (Plummer et al., 1998), and *in vivo* expression of the human epileptic encephalopathy mutation N1768D in the mouse results in a similar phenotype of early onset convulsive seizures and SUDEP (Jones and Meisler, 2014)(and unpublished observations by MHM). The 6-kb open reading frame was sequenced to confirm the absence of additional mutations.

To assess protein stability, mutant and wildtype cDNAs were transfected into HEK293 cells which are well suited

for Western blot analysis because of the lack of endogenous sodium channel protein. After culture for 24 h at 37 °C, cells were harvested and divided in half for extraction of RNA and protein. To control for transfection efficiency the abundance of the Nav1.6 transcript was analysed by qRT-PCR, as previously described (Lenk et al., 2011). Transfected cells matched for abundance of the Nav1.6 transcript were lysed in RIPA buffer and aliquots containing 30 μg of protein were incubated with Laemmli sample buffer for 20 min at 37 °C, electrophoresed through 4—15% acrylamide gradient gels (Criterion), and immunostained with rabbit polyclonal anti-Nav1.6 (Alomone ASC-009, 1:100) and, as an internal control, mouse monoclonal anti-FIG4 (NeuroMab clone N202/7).

Functional characterization of the mutant channel

Channel activity was evaluated by *co*-transfection of the eGFP cDNA together with mutant or wildtype Nav1.6 murine cDNAs into the dorsal root ganglion (DRG) neuron-derived cell line ND7/23 as previously described (Sharkey et al., 2009; Veeramah et al., 2012). ND7/23 neuronal cells support larger Nav1.6 currents than HEK293 cells, and have been our preferred expression system for voltage-clamp experiments. In the presence of 300 nM TTX, endogenous sodium currents are blocked and currents derived from the transfected Nav1.6$_R$ clones can be studied in isolation. Forty-eight hours after transfection, cells with robust green fluorescence were selected for recording. For one set of experiments, transfected ND7/23 cells were incubated overnight at 30 °C instead of 37 °C prior to recording.

Whole-cell voltage-clamp recordings were performed and analysed as previously described (Veeramah et al., 2012) (and supplement). Data were analysed using Clampfit 10.2 (Molecular Devices) and Origin 8.5 Pro (Microcal Software). The Mann—Whitney nonparametric test was used to analyse current density data. Student *t*-test was used to assess the statistical significance in characteristics of WT and NaV1.6R-Arg223Gly mutant channels.

Results

Mutation detection

Sequencing coverage was between 50 and 100× in parents and proband, with percentage of insufficiently covered target sequences ranging from 7% in the proband to 13% in the father. The patient carried a *de novo* variant in *SCN8A:* chr12:52082594 (hg19); c.667A > G, p.Arg223Gly. The mutation alters the second arginine residue in the voltage-sensing transmembrane segment S4 of domain I, and is highly conserved across species (Supp. Fig. A2).

Description of patient

The patient carrying the p.Arg223Gly mutation is the daughter of healthy unrelated parents, and was 3 years old at the latest investigation in 2013. She was born after an uneventful pregnancy of 41 weeks. At age 6 months, she developed clustered episodes of eye rolling and mouthing movements, within days evolving into clusters of flexor spasms, occurring daily with increasing frequency. The EEG showed an epileptic encephalopathy and valproic acid was started. After a few days, the EEG evolved to a hypsarhythmia and treatment with adrenocorticotropic hormone (ACTH) therapy was started, but unsuccessful, and treatment with vigabatrin was initiated. Seizure severity and duration decreased for a few days, but thereafter increased again, despite treatment with pyridoxal phosphate, nitrazepam, midazolam, levetiracetam and diphantoin. Because of the risk of respiratory insufficiency and on-going, frequent seizures characterized by eye rolling, tachypnoea and tachycardia, the patient was admitted to the intensive care unit for ventilation and treatment with subsequently phenobarbital, topiramate, propofol, thiopental, methylprednisolone and magnesium. A ketogenic diet was started. Hereafter she continued to have brief tonic and clonic seizures occurring 2 to 3 times a day.

At age six months, when seizures were first observed, development was slightly delayed. Seizure onset was associated with developmental regression. At age three years she showed severe psychomotor retardation: she was not able to sit without support and had no speech. Head circumference was normal at seizure onset (−1 SD) but showed progressive decline and at age 2.5 years it was −3 SD. Comorbid problems were central precocious puberty diagnosed at age 19 months, and constipation.

After the intensive care unit stay, EEG showed multifocal epileptiform discharges and background slowing. Magnetic resonance imaging (MRI) of the brain was initially normal but at age 9 months showed diffuse brain atrophy, including slight atrophy of the cerebellum, and interruption of myelination.

The clinical characteristics of our patient are summarized in Supplemental Table A1.

Functional characterization of the mutant channel

The p.Arg223Gly mutation was introduced into the cDNA clone mNa$_V$1.6$_R$ as described in Methods. Wildtype and mutant plasmids were transfected into the DRG-derived neuronal cell line ND7/23 and whole-cell voltage-clamp recordings were performed (Fig. 1). We used the mouse Nav1.6 clone in the present study to facilitate comparison with our previous characterization of the first *SCN8A* human mutation (Veeramah et al., 2012).

Examples of inward currents recorded by this protocol are shown in Fig. 1A. With standard culture conditions (transfected cells incubated at 37 °C), the peak current density generated by the mutant channel (-14.3 ± 3.7 *pA/pF*, $n = 15$) was greatly reduced in comparison with that of the wildtype channel (-69 ± 30 *pA/pF*, $n = 14$, $p = 0.047$) (Fig. 1B).

One possible cause of reduced current amplitude would be reduced levels of channel protein due to misfolding at 37 °C (Sharkey et al., 2009). To evaluate this possibility, we transfected HEK293 cells and examined the abundance of mutant and wildtype protein by Western blot. To control for variation in transfection efficiency, we isolated RNA from transfected cells and determined the abundance of the Nav1.6 transcript by qRT-PCR. Transfections with

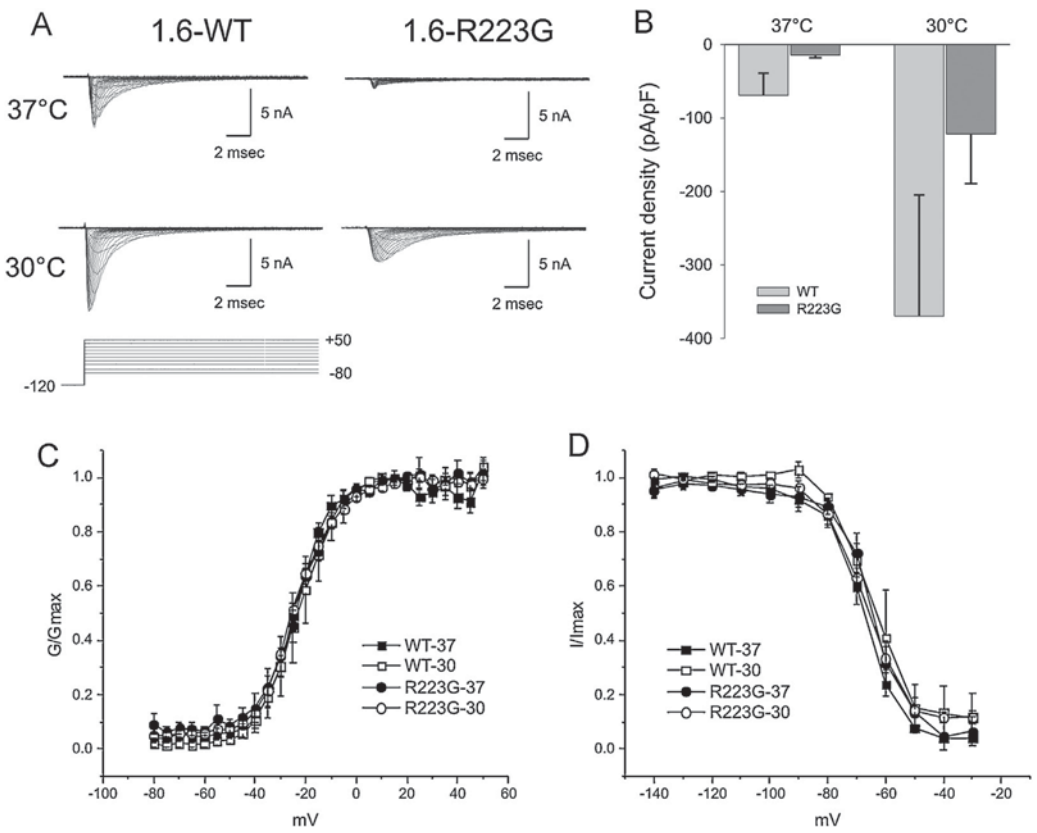

Fig. 1 *Functional characterization of the p.Arg223Gly mutant in Nav1.6.* Neuronal ND7/23 cells were transfected with wildtype or mutant Nav1.6 cDNA. (A) Cells were grown overnight at the normal temperature of 37 °C or reduced temperature of 30 °C and recorded at room temperature. Superimposed traces recorded in response to the activation stimulation protocol (100 msec duration pulses) are shown. (B) Peak currents were normalized for cell capacitance and averaged to obtain the expressed current-density for cells expressing mNav1.6r-WT (light grey, $n = 14$ at 37 °C, 9 at 30 °C) or mNav1.6r-Arg223Gly (dark grey, $n = 15$ at 37 °C, 12 at 30 °C) grown at 37 °C or 30 °C overnight. (C) Activation *G—V* curves were normalized and averaged as described in 'Methods'. (D) Responses to the fast-inactivation protocol are analysed to obtain the voltage-dependence of fast-inactivation as described in 'Methods'. Error bars are standard error of the mean (SEM). The averages of the normalized *G—V* curves for activation for Arg223Gly and WT channels grown at 37 °C or 30 °C were not significantly different (C). See Supplement for data.

comparable transcript level were compared by Western blotting. The amount of mutant protein was consistently reduced in comparison with wildtype channel in four independent transfection experiments (Fig. 3 and Supplemental Fig. A3). The amount of mutant channel in 50 μg of transfected cell extract was comparable to the level of wildtype protein in 10 μg of extract, suggesting that the stability of the mutant protein is reduced by 80% (Supplemental Fig. A3, left panel).

To compensate for the defect in expression of mutant channel protein at 37 °C, we cultured transfected ND7/23 cells at 30 °C. This resulted in significant recovery of channel function (Fig. 1A). At 30 °C, the peak current density measured from cells transfected with p.Arg223Gly (-122 ± 67 *pA/pF*, $n = 12$) was approximately one third of the current density of wildtype-transfected cells (-370 ± 165 *pA/pF*, $n = 9$, $p = 0.014$) (Fig. 1B).

The voltage-dependence of activation and fast-inactivation were examined by transforming the peak current *versus* voltage (*I—V*) curves into conductance *versus* voltage (*G—V*) curves. The Boltzmann fits for both activation and fast-inactivation were derived for each cell individually. The averages of the normalized *G—V* curves for activation for p.Arg223Gly and WT channels grown at 37 °C or 30 °C were not significantly different (Fig. 1C). Growth at 37 °C *versus* 30 °C did not significantly affect the average of the fits for fast-inactivation (Fig. 1D).

We evaluated the response of wildtype and mutant channels to slow ramp depolarisations. These experiments were carried out at 30 °C to stabilize the mutant protein. To permit comparisons between cells, the response was normalized to the peak inward current recorded during the activation *I—V* protocol. The averaged response of mutant and wildtype channels is shown in Fig. 2. The peak of the slow ramp response of cells expressing p.Arg223Gly averaged $3.5 \pm 0.7\%$ ($n = 11$), which is a 3-fold increase over the average ramp response of $1.0 \pm 0.2\%$ in WT-expressing cells ($n = 5$, $p = 0.004$).

Discussion

We describe a patient with epileptic encephalopathy who carries a *de novo* missense variant in *SCN8A*

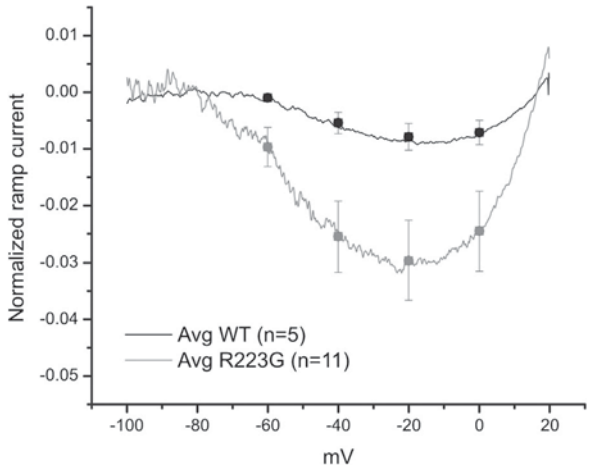

Fig. 2 *Enhanced ramp activity of Nav1.6 resulting from the p.Arg223Gly mutation.* Data traces recorded in response to a slow ramp stimulus of −120 mV to +20 mV over 600 ms are filtered to 200 Hz and normalized to peak *I*—*V* current. The normalized ramp traces are averaged together for cells expressing Nav1.6-WT (black line, $n = 5$) or Nav1.6-Arg223Gly channels (grey line, $n = 11$). Selected points are plotted as mean ± SEM to indicate the variance of the averages. (For interpretation of the references to color in this figure legend, the reader is referred to the web version of this article.)

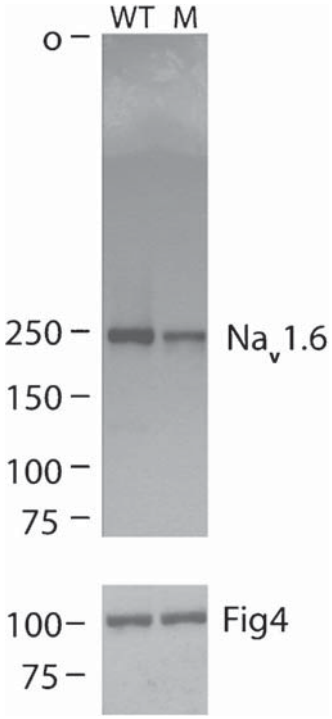

Fig. 3 *The p.Arg223Gly mutation reduces the stability of the Nav1.6 channel protein.* HEK293 cells were transfected with mutant or wildtype Nav1.6 cDNA and cultured for 24 h at 37 degrees. Aliquots of cell extracts containing 30 μg protein were subjected to electrophoresis on 4—15% gradient gels and transferred to a nitrocellulose filter as described in 'Methods'. Nav1.6 was detected with a rabbit polyclonal antibody (Alomone). As a control for loading and transfer efficiency, the filter was washed and the endogenous FIG4 protein was immunostained with a mouse monoclonal antibody (NeuroMab). Mu, mutant; Wt, wildtype; Un, untransfected; o, gel origin.

(Nav1.6 p.Arg223Gly) and compared clinical phenotype and biophysical properties of the mutation with a previous described mutation (Veeramah et al., 2012). The two patients exhibit similar clinical features including severe epileptic encephalopathy with onset at age 6 months. Unlike in Dravet syndrome, initial seizures showed no association with fever or illness. Initial seizure frequency was very high in both patients. However, the clinical progression is more severe in the current patient, since at the age of 3 years the original patient was ambulatory with less cognitive impairment. In both patients, the clinical picture includes spasms, albeit at different ages, and developmental delay with poor outcome (Supp. Table 1A). Comparison of the novel Nav1.6 Arg223Gly mutation with the previously described Nav1.6 Asn1768Asp demonstrated that the effects of the two mutations are divergent in several respects. First, the Arg223Gly current amplitude was only about 20% that of the wild type channels when cells were incubated at the physiological temperature of 37 °C. Second, Arg223Gly mutant channels do not produce a persistent current or manifest incomplete inactivation as observed in Nav1.6 Asn1768Asp current recordings. Third, at the permissive temperature of 30 °C we observed a 3-fold increase in the ramp current normalized to peak current for Nav1.6 Arg223Gly, similar to that observed for Nav1.6 Asn1768Asp. However, when expressed in terms of absolute current levels, there was a significant reduction in ramp current of the mutant channel even at the permissive temperature, suggesting that this increase may not be biologically relevant. These observations argue that a loss-of-function mutation in *SCN8A* may underlie the seizure disorder in this patient

At 37 °C peak-current density was significantly reduced in Nav1.6 Arg223Gly, which may be explained by the reduced protein stability of the mutant relative to WT. At 30 °C, peak-currents were partially recovered, an effect seen in other ion channel mutants, which may make gain of function effects more apparent (Cestele et al., 2013). Though 37 °C is the physiological temperature for humans, *in vitro* systems may display a higher instability at these temperatures than the *in vivo* situation owing to their artificial nature. Furthermore, *in vivo* compensation for the reduced *SCN8A* activity might also contribute to neuronal hyperexcitability (Cestele et al., 2013; Vega et al., 2008). However, unlike the Nav1.1 mutation referred to above (Cestele et al., 2013) and the folding-defective Nav1.6 mutation in ataxia3 mice (Sharkey et al., 2009), the rescue of p.Arg223Gly at the lower temperature did not uncover a robust gain-of-function change that could explain the hyperexcitability phenotype.

Multiple biophysical mechanisms can contribute to the production of the ramp current (Estacion and Waxman, 2013). Although window currents generated within the voltage domain delineated by the Boltzmann's fits for activation and inactivation may contribute to ramp currents, other properties, for example the rate of entry into closed state inactivation, may have a major effect (Cummins et al., 1998). Thus, an increased ramp current may occur in the absence of an effect on the voltage-dependence of inactivation. At the cellular level, a significant increase in ramp

currents may enhance the activity of the mutant channel in the range of subthreshold depolarisations for wildtype channels, and thus enhance the probability of neurons reaching the threshold for action potential firing. However, although we report an increase in the ramp current normalized to the peak current, we note that the large and significant reduction in the peak current density of the Arg223Gly channels, reaching only 20% that of wildtype channels at physiological temperatures, suggests that, in terms of absolute currents, the mutant channel may only produce up to 60% of the ramp current of the wildtype channel.

Mutations in *SCN1A* cause the epileptic encephalopathy Dravet syndrome (MIM 607208). Most of the pathogenic *SCN1A* mutations cause loss-of-function (Claes et al., 2009). Mutations in *SCN2A* causing epileptic encephalopathy (MIM #613721) include both loss- and gain-of-function mutations (Ogiwara et al., 2009). The previously described *SCN8A* mutation was a gain-of-function mutation (Veeramah et al., 2012), and all of the described *SCN8A* mutations thus far have been missense mutations which could cause gain or loss of function. The alpha subunits of different sodium channels have distinct intracellular and anatomical distributions in the brain. In a recent review, Oliva et al. (2012) compared the role of these voltage-gated sodium channels. The three major subunits, *SCN1A*, *SCN2A*, and *SCN8A*, are all expressed in excitatory neurons (Liu et al., 2013; Ogiwara et al., 2013; Oliva et al., 2012). *SCN1A* and *SCN8A* are also expressed in inhibitory neurons (Cheah et al., 2012; Dutton et al., 2012; Lorincz and Nusser, 2008; Ogiwara et al., 2013). All three channel proteins are present in specific domains of the axon initial segment, where *SCN2A* may contribute to back propagation to the soma and dendrites (Oliva et al., 2012, 2014). *SCN8A* encoded Nav1.6 is concentrated in the distal portion of the axon initial segment (AIS) and in the nodes of Ranvier (Lorincz and Nusser, 2008; Royeck et al., 2008; Van Wart and Matthews, 2006) and is also found at lower abundance in the soma and dendrites (Lorincz and Nusser, 2008, 2010). *SCN8A* has a lower threshold of activation than *SCN2A* (Royeck et al., 2008; Rush et al., 2005), and plays an important role in action potential initiation (Hu et al., 2009). Though strong similarities exist between these closely related channels, there are important functional differences. Mutations in all three channels can result in epilepsy, but the biophysical mechanisms are probably different and need careful examination.

We previously demonstrated that a gain-of-function mutation of Nav1.6 from a subject with infantile-onset epilepsy enhances persistent sodium current and shifts fast-inactivation in a depolarizing direction, producing hyperexcitability and PDS-like complexes in pyramidal hippocampal neurons (Veeramah et al., 2012). Studies on *Scn8a*^{med} mice lacking functional Nav1.6 channels demonstrate reduced excitability of CA1 pyramidal neurons (Royeck et al., 2008). Up-regulation of Nav1.6 by the splicing factor Celf4, which is expressed in excitatory but not inhibitory neurons, has been linked to seizures (Sun et al., 2013). Nevertheless, loss-of-function Nav1.6 might lead to differential impact on inhibitory neurons, where Nav1.6 is known to be present at the axon initial segment (Lorincz and Nusser, 2008), possibly affecting inhibitory neurons more than excitatory neurons within an epileptogenic circuit. The heterozygous Scn8a-null mouse has in fact been reported to manifest spontaneous spike-wave discharges consistent with absence epilepsy (Papale et al., 2009). Variation in other ion channels may also influence the disease phenotype in an individual patient. Thus a loss-of-function mutation in Nav1.6, as shown in this study, might yield an epileptic phenotype.

It remains to be determined whether pure loss-of-function mutations in human *SCN8A* are a common cause of epileptic encephalopathy. It is clear that heterozygous loss-of-function of *SCN8A* is not invariably associated with epilepsy. For example, the frameshift mutation p.Pro1719Arg*6 segregates in a family with mild cognitive impairment but no history of seizures (Trudeau et al., 2006). In addition, the heterozygous protein truncation variant P.Gly656Arg is present in 14/5300 individuals in the exome variant server database (Exome Variant Server, NHLBI GO Exome Sequencing Project (ESP), Seattle, WA (URL: http://evs.gs.washington.edu/EVS/) [March, 2014 accessed].) which does not include individuals with early onset neurological disorders. The effect of loss-of-function mutations is likely to be influenced by genetic background of each individual genome (Oliva et al., 2014), in particular by variation in other channel genes.

The patient described here supports recent reports that *de novo* mutations of *SCN8A* constitute a recurrent cause of severe, early onset epileptic encephalopathy. The functional data demonstrate that the *SCN8A*-p.Arg223Gly mutation in this mutation is deleterious, although the precise mechanism of epileptogenesis is not completely established. Functional characterization of additional variants in addition to the two reported to date will contribute to understanding the genotype—phenotype correlations and the mechanisms underlying this devastating disorder.

Note added in proof

While this paper was under review, a paper describing functional characterization of mutation p.Thr767Ile in SCN8A, which had also been found in a patient with epileptic encephalopathy, came out. This mutation shows different functional characteristics than the mutation described here (Estacion et al., 2014).

Funding

MHM was supported by NIH Grant NS34509 and JEO by T32 GM007544 and the Rackham School of Graduate Studies, University of Michigan. SGW and SDH are supported in part by grants from the Rehabilitation Research Service (SDH and SGW: B3141-C and B7623-R) and Medical Research Service (SGW: CC103), Department of Veterans Affairs, USA. CGFdK and BPCK are supported by NEF (Nationaal Epilepsie Fonds) grant 10.09.

Acknowledgements

We thank the families for their cooperation.

Appendix A. Supplementary data

Supplementary data associated with this article can be found, in the online version, at http://dx.doi.org/10.1016/j.eplepsyres.2014.08.020.

References

Carvill, G.L., Heavin, S.B., Yendle, S.C., McMahon, J.M., O'Roak, B.J., Cook, J., Khan, A., Dorschner, M.O., Weaver, M., Calvert, S., Malone, S., Wallace, G., Stanley, T., Bye, A.M., Bleasel, A., Howell, K.B., Kivity, S., Mackay, M.T., Rodriguez-Casero, V., Webster, R., Korczyn, A., Afawi, Z., Zelnick, N., Lerman-Sagie, T., Lev, D., Moller, R.S., Gill, D., Andrade, D.M., Freeman, J.L., Sadleir, L.G., Shendure, J., Berkovic, S.F., Scheffer, I.E., Mefford, H.C., 2013. Targeted resequencing in epileptic encephalopathies identifies de novo mutations in CHD2 and SYNGAP1. Nat. Genet. 45, 825—830.

Cestele, S., Schiavon, E., Rusconi, R., Franceschetti, S., Mantegazza, M., 2013. Nonfunctional NaV1.1 familial hemiplegic migraine mutant transformed into gain of function by partial rescue of folding defects. Proc. Natl. Acad. Sci. U.S.A. 110, 17546—17551.

Cheah, C.S., Yu, F.H., Westenbroek, R.E., Kalume, F.K., Oakley, J.C., Potter, G.B., Rubenstein, J.L., Catterall, W.A., 2012. Specific deletion of NaV1.1 sodium channels in inhibitory interneurons causes seizures and premature death in a mouse model of Dravet syndrome. Proc. Natl. Acad. Sci. U.S.A. 109, 14646—14651.

Claes, L.R., Deprez, L., Suls, A., Baets, J., Smets, K., Van Dyck, T., Deconinck, T., Jordanova, A., De Jonghe, P., 2009. The SCN1A variant database: a novel research and diagnostic tool. Hum. Mutat. 30, E904—E920.

Cummins, T.R., Howe, J.R., Waxman, S.G., 1998. Slow closed-state inactivation: a novel mechanism underlying ramp currents in cells expressing the hNE/PN1 sodium channel. J. Neurosci. 18, 9607—9619.

Dutton, S.B., Makinson, C.D., Papale, L.A., Shankar, A., Balakrishnan, B., Nakazawa, K., Escayg, A., 2012. Preferential inactivation of Scn1a in parvalbumin interneurons increases seizure susceptibility. Neurobiol. Dis. 49C, 211—220.

Epi4K-Consortium, Epilepsy Phenome/Genome, P., Allen, A.S., Berkovic, S.F., Cossette, P., Delanty, N., Dlugos, D., Eichler, E.E., Epstein, M.P., Glauser, T., Goldstein, D.B., Han, Y., Heinzen, E.L., Hitomi, Y., Howell, K.B., Johnson, M.R., Kuzniecky, R., Lowenstein, D.H., Lu, Y.F., Madou, M.R., Marson, A.G., Mefford, H.C., Esmaeeli Nieh, S., O'Brien, T.J., Ottman, R., Petrovski, S., Poduri, A., Ruzzo, E.K., Scheffer, I.E., Sherr, E.H., Yuskaitis, C.J., Abou-Khalil, B., Alldredge, B.K., Bautista, J.F., Berkovic, S.F., Boro, A., Cascino, G.D., Consalvo, D., Crumrine, P., Devinsky, O., Dlugos, D., Epstein, M.P., Fiol, M., Fountain, N.B., French, J., Friedman, D., Geller, E.B., Glauser, T., Glynn, S., Haut, S.R., Hayward, J., Helmers, S.L., Joshi, S., Kanner, A., Kirsch, H.E., Knowlton, R.C., Kossoff, E.H., Kuperman, R., Kuzniecky, R., Lowenstein, D.H., McGuire, S.M., Motika, P.V., Novotny, E.J., Ottman, R., Paolicchi, J.M., Parent, J.M., Park, K., Poduri, A., Scheffer, I.E., Shellhaas, R.A., Sherr, E.H., Shih, J.J., Singh, R., Sirven, J., Smith, M.C., Sullivan, J., Lin Thio, L., Venkat, A., Vining, E.P., Von Allmen, G.K., Weisenberg, J.L., Widdess-Walsh, P., Winawer, M.R., 2013. De novo mutations in epileptic encephalopathies. Nature 501, 217—221.

Estacion, M., O'Brien, J.E., Conravey, A., Hammer, M.F., Waxman, S.G., Dib-Hajj, S.D., Meisler, M.H., 2014. A novel de novo mutation of SCN8A (Nav1.6) with enhanced channel activation in a child with epileptic encephalopathy. Neurobiol Dis. 45, 117—123.

Estacion, M., Waxman, S.G., 2013. The response of Na(V)1.3 sodium channels to ramp stimuli: multiple components and mechanisms. J. Neurophysiol. 109, 306—314.

Hu, W., Tian, C., Li, T., Yang, M., Hou, H., Shu, Y., 2009. Distinct contributions of Na(v)1.6 and Na(v)1.2 in action potential initiation and backpropagation. Nat. Neurosci. 12, 996—1002.

Jones, J.M., Meisler, M.H., 2014. Modeling human epilepsy by TALEN targeting of mouse sodium channel Scn8a. Genesis 52, 141—148.

Lenk, G.M., Ferguson, C.J., Chow, C.Y., Jin, N., Jones, J.M., Grant, A.E., Zolov, S.N., Winters, J.J., Giger, R.J., Dowling, J.J., Weisman, L.S., Meisler, M.H., 2011. Pathogenic mechanism of the FIG4 mutation responsible for Charcot—Marie—-Tooth disease CMT4J. PLoS Genet. 7, e1002104.

Liu, Y., Lopez-Santiago, L.F., Yuan, Y., Jones, J.M., Zhang, H., O'Malley, H.A., Patino, G.A., O'Brien, J.E., Rusconi, R., Gupta, A., Thompson, R.C., Natowicz, M.R., Meisler, M.H., Isom, L.L., Parent, J.M., 2013. Dravet syndrome patient-derived neurons suggest a novel epilepsy mechanism. Ann. Neurol. 74, 128—139.

Lorincz, A., Nusser, Z., 2008. Cell-type-dependent molecular composition of the axon initial segment. J. Neurosci. 28, 14329—14340.

Lorincz, A., Nusser, Z., 2010. Molecular identity of dendritic voltage-gated sodium channels. Science 328, 906—909.

Meisler, M.H., O'Brien, J.E., Sharkey, L.M., 2010. Sodium channel gene family: epilepsy mutations, gene interactions and modifier effects. J. Physiol. 588, 1841—1848.

Meisler, M.H., Kearney, J.A., 2005. Sodium channel mutations in epilepsy and other neurological disorders. J. Clin. Invest. 115, 2010—2017.

Mulley, J.C., Scheffer, I.E., Petrou, S., Dibbens, L.M., Berkovic, S.F., Harkin, L.A., 2005. SCN1A mutations and epilepsy. Hum. Mutat. 25, 535—542.

Nijman, I.J., Mokry, M., van Boxtel, R., Toonen, P., de Bruijn, E., Cuppen, E., 2010. Mutation discovery by targeted genomic enrichment of multiplexed barcoded samples. Nat. Methods 7, 913—915.

O'Brien, J.E., Meisler, M.H., 2013. Sodium channel (Na1.6): properties and mutations in epileptic encephalopathy and intellectual disability. Front. Genet. 4, 213.

Ogiwara, I., Ito, K., Sawaishi, Y., Osaka, H., Mazaki, E., Inoue, I., Montal, M., Hashikawa, T., Shike, T., Fujiwara, T., Inoue, Y., Kaneda, M., Yamakawa, K., 2009. De novo mutations of voltage-gated sodium channel alphaII gene SCN2A in intractable epilepsies. Neurology 73, 1046—1053.

Ogiwara, I., Iwasato, T., Miyamoto, H., Iwata, R., Yamagata, T., Mazaki, E., Yanagawa, Y., Tamamaki, N., Hensch, T.K., Itohara, S., Yamakawa, K., 2013. Nav1.1 haploinsufficiency in excitatory neurons ameliorates seizure-associated sudden death in a mouse model of Dravet syndrome. Hum. Mol. Genet. 22, 4784—4804.

Oliva, M., Berkovic, S.F., Petrou, S., 2012. Sodium channels and the neurobiology of epilepsy. Epilepsia 53, 1849—1859.

Oliva, M.K., McGarr, T.C., Beyer, B.J., Gazina, E., Kaplan, D.I., Cordeiro, L., Thomas, E., Dib-Hajj, S.D., Waxman, S.G., Frankel, W.N., Petrou, S., 2014. Physiological and genetic analysis of multiple sodium channel variants in a model of genetic absence epilepsy. Neurobiol. Dis 67, 180—190.

Papale, L.A., Beyer, B., Jones, J.M., Sharkey, L.M., Tufik, S., Epstein, M., Letts, V.A., Meisler, M.H., Frankel, W.N., Escayg, A., 2009. Heterozygous mutations of the voltage-gated sodium channel SCN8A are associated with spike-wave discharges and absence epilepsy in mice. Hum. Mol. Genet. 18, 1633—1641.

Plummer, N.W., Galt, J., Jones, J.M., Burgess, D.L., Sprunger, L.K., Kohrman, D.C., Meisler, M.H., 1998. Exon organization, coding sequence, physical mapping, and polymorphic intragenic markers for the human neuronal sodium channel gene SCN8A. Genomics 54, 287—296.

Rauch, A., Wieczorek, D., Graf, E., Wieland, T., Endele, S., Schwarzmayr, T., Albrecht, B., Bartholdi, D., Beygo, J., Di Donato, N., Dufke, A., Cremer, K., Hempel, M., Horn, D., Hoyer, J., Joset, P., Ropke, A., Moog, U., Riess, A., Thiel, C.T., Tzschach, A., Wiesener, A., Wohlleber, E., Zweier, C., Ekici, A.B., Zink, A.M., Rump, A., Meisinger, C., Grallert, H., Sticht, H., Schenck, A., Engels, H., Rappold, G., Schrock, E., Wieacker, P., Riess, O., Meitinger, T., Reis, A., Strom, T.M., 2012. Range of genetic mutations associated with severe non-syndromic

sporadic intellectual disability: an exome sequencing study. Lancet 380, 1674—1682.

Royeck, M., Horstmann, M.T., Remy, S., Reitze, M., Yaari, Y., Beck, H., 2008. Role of axonal NaV1.6 sodium channels in action potential initiation of CA1 pyramidal neurons. J. Neurophysiol. 100, 2361—2380.

Rush, A.M., Dib-Hajj, S.D., Waxman, S.G., 2005. Electrophysiological properties of two axonal sodium channels, Nav1.2 and Nav1.6, expressed in mouse spinal sensory neurones. J. Physiol. 564, 803—815.

Scheffer, I.E., Zhang, Y.H., Jansen, F.E., Dibbens, L., 2009. Dravet syndrome or genetic (generalized) epilepsy with febrile seizures plus? Brain Dev. 31, 394—400.

Sharkey, L.M., Cheng, X., Drews, V., Buchner, D.A., Jones, J.M., Justice, M.J., Waxman, S.G., Dib-Hajj, S.D., Meisler, M.H., 2009. The ataxia3 mutation in the N-terminal cytoplasmic domain of sodium channel $Na_v1.6$ disrupts intracellular trafficking. J. Neurosci. 29, 2733—2741.

Shi, X., Yasumoto, S., Kurahashi, H., Nakagawa, E., Fukasawa, T., Uchiya, S., Hirose, S., 2012. Clinical spectrum of SCN2A mutations. Brain Dev. 34, 541—545.

Sun, W., Wagnon, J.L., Mahaffey, C.L., Briese, M., Ule, J., Frankel, W.N., 2013. Aberrant sodium channel activity in the complex seizure disorder of Celf4 mutant mice. J. Physiol. 591, 241—255.

Trudeau, M.M., Dalton, J.C., Day, J.W., Ranum, L.P., Meisler, M.H., 2006. Heterozygosity for a protein truncation mutation of sodium channel SCN8A in a patient with cerebellar atrophy, ataxia, and mental retardation. J. Med. Genet. 43, 527—530.

Vaher, U., Noukas, M., Nikopensius, T., Kals, M., Annilo, T., Nelis, M., Ounap, K., Reimand, T., Talvik, I., Ilves, P., Piirsoo, A., Seppet, E., Metspalu, A., Talvik, T., 2013. De Novo SCN8A mutation identified by whole-exome sequencing in a boy with neonatal epileptic encephalopathy, multiple congenital anomalies, and movement disorders. J. Child Neurol., Epub ahead of print.

Van Wart, A., Matthews, G., 2006. Impaired firing and cell-specific compensation in neurons lacking Nav1.6 sodium channels. J. Neurosci. 26, 7172—7180.

Veeramah, K.R., O'Brien, J.E., Meisler, M.H., Cheng, X., Dib-Hajj, S.D., Waxman, S.G., Talwar, D., Girirajan, S., Eichler, E.E., Restifo, L.L., Erickson, R.P., Hammer, M.F., 2012. De novo pathogenic SCN8A mutation identified by whole-genome sequencing of a family quartet affected by infantile epileptic encephalopathy and SUDEP. Am. J. Hum. Genet. 90, 502—510.

Vega, A.V., Henry, D.L., Matthews, G., 2008. Reduced expression of Na(v)1.6 sodium channels and compensation by Na(v)1.2 channels in mice heterozygous for a null mutation in Scn8a. Neurosci. Lett. 442, 69—73.